Quadratic power corrections to the dynamic magnetization using the transverse magnetostatic wave-optical interaction

A. Prabhakar, and D. D. Stancil

Citation: Journal of Applied Physics **81**, 2730 (1997);
View online: https://doi.org/10.1063/1.363970
View Table of Contents: http://aip.scitation.org/toc/jap/81/6
Published by the American Institute of Physics

Quadratic power corrections to the dynamic magnetization using the transverse magnetostatic wave-optical interaction

A. Prabhakar[a)]
Department of Physics, Carnegie Mellon University, Pittsburgh, Pennsylvania 15213

D. D. Stancil
Electrical and Computer Engineering, Carnegie Mellon University, Pittsburgh, Pennsylvania 15213

(Received 11 November 1996; accepted for publication 3 December 1996)

A microstrip T-transducer excites forward volume magnetostatic waves (MSWs) in a $[BiLu]_3Fe_5O_{12}$ film. An optical beam is edge coupled into the film and the transverse MSW–optical interaction is observed at high microwave power levels. Using the coupled mode equations, we demonstrate that a T-transducer causes the intensity of the diffracted beam to be a product of terms involving the magneto-optic coupling coefficient (κ) and the phase mismatch between the optical guided modes and the MSWs. Taylor series expansions for κ and the MSW wave number (β) are used to obtain an analytic expression for the MSW–optical interaction. The dependence on β causes a shift in the interaction spectrum with increasing power. After correcting for this shift, the residual dependence on power is attributed to a quadratic correction to the dynamic magnetization which in turn affects κ. We demonstrate how the quadratic dependence plays an important role in accurately determining an expansion for the MSW dispersion relation. © *1997 American Institute of Physics.* [S0021-8979(97)02606-6]

I. INTRODUCTION

The interaction between optical guided modes and magnetostatic waves (MSWs) was observed over a decade ago[1,2] and is now well documented. At low microwave power levels, the dynamic magnetization is usually described by the linear approximation to the Landau–Lifshitz equation. As we increase the input microwave power, the increase in dynamic magnetization causes a reduction in the demagnetizing field and a subsequent shift in the microwave passband. Such a shift was reported in experiments on MSW delay lines[3] and in the transverse MSW–optical interaction.[4] This phenomenon was explained by the inclusion of the lowest order nonlinear terms in the Landau–Lifshitz equation.

In the present experiment, we use the transverse MSW–optical interaction to determine the quadratic coefficients in a Taylor series expansion for the magneto-optic coupling coefficient (κ). Such a study is facilitated by the use of a microstrip T-shaped transducer instead of the conventionally used L-shaped transducer. We solve the coupled-mode equations for the new geometry in Sec. II. After correcting for the effects of the lowest order nonlinear terms, the residual dependence of the MSW–optical interaction on microwave power is attributed to the next higher order term in the Taylor series. In Sec. III we analyze our experimental data and measure the quadratic coefficient in the Taylor series.

In the presence of high microwave power, there can be a significant change in the temperature of the film. This causes a reduction in the demagnetizing field which results in a shift in the microwave passband. This shift is similar to that observed by the inclusion of the lowest order nonlinear terms in the MSW dispersion relation. In Sec. IV we build a simple heuristic model that allows us to estimate the effects of thermal demagnetization under steady state conditions.

It was recently shown that the third order derivative with respect to wave number in the MSW dispersion relation has a significant effect on the propagation of MSW envelope solitons.[5] Likewise, it is conceivable that as we increase microwave power, researchers will begin to observe a nonlinear dependence on power in the dispersion relation. The quadratic coefficient in an expansion for κ is a direct measure of the quadratic dependence of the dynamic magnetization on input power. The MSW–optical interaction allows us to estimate the second order power dependence in a Taylor series expansion for the edge of the MSW passband. A typical calculation is shown in Sec. V.

This technique of measuring the change in dynamic magnetization is possible only in films with a large ferromagnetic linewidth and having a high threshold for the excitation of parametric spin waves. The study of MSW–optical interactions in the presence of parametric spin waves is more complicated and has been addressed by other researchers.[6]

II. THEORY OF MSW–OPTICAL INTERACTION

A schematic of the experimental setup is shown in Fig. 1 and is used as a basis for our theoretical model. A TM polarized optical beam is edge coupled into a $Bi_{0.8}Lu_{2.2}Fe_5O_{12}$ film of thickness 6.3 μm. Forward volume MSWs are excited by placing the film in physical contact with a T-transducer. The transducer has a total length ($2L$) of 1 cm, a width of $\sim$50 μm and is deposited on a 250 μm Alumina substrate. The microwave signal is modulated using a low frequency square wave which in turn is used by a lock-in amplifier as a reference signal to monitor the intensity of the TE polarized light. This seemingly complicated T-transducer structure serves a definite purpose. The MSWs excited by each arm of the transducer have a relative phase shift of 180°, resulting in somewhat unusual device characteristics. The rest of this section is devoted to developing a

a)Electronic mail:anilp@cmu.edu

 0021-8979/97/81(6)/2730/6/$10.00

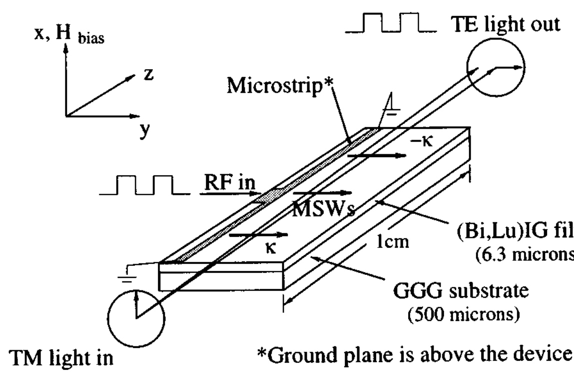

FIG. 1. Transverse MSW–optical interaction geometry using a T-transducer. The sign of the coupling coefficient changes as the optical modes cross the center of the transducer.

theoretical foundation for the MSW–optical interaction and its dependence on the microwave power fed into the T-transducer. Subsequent sections will deal with the interpretation of our experimental observations based on this theory.

A. Coupled mode theory

The interaction between optical guided modes and propagating MSWs can be described by the coupled mode equations.[7] If we identify the input amplitude of the TM light as A_0 and that of the TE light as B_0, the solutions to the coupled mode equations for an interaction length z are[8]

$$\begin{aligned} A(z) &= f(A_0,B_0,\kappa,\Delta,z) \\ &= e^{-i\Delta z/2}\left(A_0 \cos \beta_0 z + \frac{\kappa B_0 + (i\Delta/2)A_0}{\beta_0} \sin \beta_0 z\right), \\ B(z) &= g(A_0,B_0,\kappa,\Delta,z) \\ &= e^{i\Delta z/2}\left(B_0 \cos \beta_0 z + \frac{-\kappa A_0 - (i\Delta/2)B_0}{\beta_0} \sin \beta_0 z\right), \end{aligned} \tag{1}$$

where $\Delta = [\boldsymbol{\beta}_A - \boldsymbol{\beta}_B \mp \boldsymbol{\beta}_{MSW}]\cdot\hat{z}$ is the phase mismatch with β corresponding to the wave number for a respective wave (as denoted by the subscript), κ is the coupling coefficient and $\beta_0 = \sqrt{\kappa^2 + (\Delta/2)^2}$.

Due to the relative phase shift of 180° between the MSWs excited by each arm of the transducer, $\kappa \rightarrow -\kappa$ as the optical beam propagates from one region of the film to another. This process has been shown schematically in Fig. 1. We obtain the solutions for the MSW–optical interaction employing a T-transducer by evaluating (1) with the following boundary conditions:

$$\begin{aligned} &A(0)=1,\ B(0)=0, \\ &A(L)=f(A(0),B(0),\kappa,\Delta,L), \\ &B(L)=g(A(0),B(0),\kappa,\Delta,L), \\ &B(2L)=g(A(L),B(L),-\kappa,\Delta,L), \end{aligned} \tag{2}$$

where f and g were defined in (1). The resulting intensity of the diffracted TE beam is given by

$$\begin{aligned} |B(2L)|^2 = \frac{\kappa^2}{\beta_0^2} \sin^2(2\beta_0 L)\bigg(&\frac{\Delta}{\beta_0}\sin(2\beta_0 L)\cos(\Delta L) \\ &- 2\cos(2\beta_0 L)\sin(\Delta L)\bigg)^2. \end{aligned} \tag{3}$$

Using the approximations $\sin(x)\approx x-(x^3/6)$ and $\cos(x)\approx 1-(x^2/2)$, we find that the lowest order terms in ΔL vanish and $|B(2L)|^2 \rightarrow 0$. This result is also intuitively sound. When $\Delta=0$, we expect the Faraday rotation in the two segments of the film to counteract and yield no net interaction signal. To analyze the behavior of the device, we retain the lowest order nonzero terms in ΔL. The above approximations to the trigonometric functions yield errors less than 10% even as $x \rightarrow \pi/3$. The output optical intensity is found to be

$$I = |B(2L)|^2 \propto \kappa^2 |\Delta|^6 L^8. \tag{4}$$

It is worthwhile to note that in a similar analysis for the commonly used L-shaped transducer, the lowest order nonzero terms do not give us a dependence on Δ. The T-structure allows us to exploit the inherent dependence of I on the input microwave power via the $\boldsymbol{\beta}_{MSW}\cdot\hat{z}$ term in Δ. This added freedom does however come at the cost of a reduction in the efficiency of the MSW–optical interaction.

B. Microwave power dependence

We shall now address the question of how the intensity of the diffracted optical beam changes with an increase in input microwave power. In a film with ϕ_F and ϕ_{CM} as the Faraday and Cotton–Mouton rotations, respectively, saturation magnetization M_s and dynamic magnetization $m_\rho = \sqrt{m_y^2 + m_z^2}$, the coupling coefficient is given by[9]

$$|\kappa| = \frac{1}{2}|\phi_F - \phi_{CM}|\frac{m_\rho}{M_s} \equiv \lambda m_\rho. \tag{5}$$

This expression for $|\kappa|$ is accurate to $O(m_\rho)$. In the appendix, we calculate the $O(m_\rho^2)$ correction to (5) for our experiment and show that it can be neglected under the approximations of (i) a constant magnetization through the thickness of the film and (ii) circularly polarized MSWs. Using the ortho-normalization of MSW modes, m_ρ can be expressed in terms of the frequency ω and the microwave power P (in mW/mm) as[8]

$$m_\rho = \frac{2}{d}\sqrt{\frac{2P}{\omega\mu_0}} \equiv \tau\sqrt{P}. \tag{6}$$

Here P is the power per unit length coupled into MSWs on either side of the transducer and is half the total power fed into a perfectly matched bidirectional transducer. Since the above equation is true only when $m_\rho \ll M_s$, we expect to observe deviations from this behavior as we arbitrarily increase P. We introduce the phenomenological parameter ξ (with units of mm/mW) so that m_ρ^2 now has a nonlinear power dependence of the form

$$m_\rho^2 = \tau^2 P(1+\xi P). \tag{7}$$

With $|\kappa|^2=\lambda^2 m_\rho^2$ we can monitor the deviations from the linear power dependence using a Taylor series expansion near (P_0,ω_0). With $\delta p=P-P_0$, $\delta\omega=\omega-\omega_0$ and $\tau_0=\tau(\omega_0)$, we find

$$\frac{|\kappa|^2}{P}=\lambda^2\tau_0^2\left(1+\xi\delta p-\frac{\delta\omega}{\omega_0}(1+\xi P_0)\right)+O[(\delta p)^2,(\delta\omega)^2]. \quad (8)$$

We can also expand the phase mismatch Δ in a Taylor series, keeping β_{TE} and β_{TM} fixed, to obtain

$$\Delta=\Delta_0-\beta_P\delta p-\beta_\omega\delta\omega+O[(\delta p)^2], \quad (9)$$

where $\Delta_0=\Delta(P_0,\omega_0)$, $\beta_P=(\partial\beta/\partial P)_\omega$, $\beta_\omega=(\partial\beta/\partial\omega)_P$ and $\beta=\beta_{MSW}$. We define a normalized output optical intensity $I'\propto I/P$ and combine (4), (8) and (9) to find

$$I'=\lambda^2\tau_0^2\left(1+\xi\delta p-\frac{\delta\omega}{\omega_0}(1+\xi P_0)\right)[\Delta_0^6-6\Delta_0^5(\beta_P\delta p+\beta_\omega\delta\omega)]+O[(\delta p)^2]. \quad (10)$$

The $\beta_P\delta p$ term in (10) causes the MSW–optical interaction spectrum to shift towards higher frequencies as we increase microwave power. This shift was observed by Cash and Stancil[4] and was explained by the inclusion of $O(\delta p)$ terms in the MSW dispersion relation. The lower edge of the MSW passband shifts linearly with power and the shift is given by

$$\delta\omega=\left(\frac{\partial\omega}{\partial P}\right)_\beta\delta p\equiv\omega_P\delta p. \quad (11)$$

ω_P is usually calculated from the MSW dispersion relation and is found to be[4]

$$\omega_P=\frac{4\omega_M}{\omega_0\mu_0 M_s^2 d^2}, \quad (12)$$

where $\omega_M=-\gamma\mu_0 M_s$ and $\gamma=-2\pi(28\ \text{GHz/T})$. This expression does not account for a change in M_s due to a thermal demagnetization of the film. In Sec. IV, we shall build a heuristic model to estimate the thermal effects.

If we follow the line $\omega=\omega_0+\omega_P\delta p$, we are following the $O(\delta p)$ shift in the passband with increasing power. Since β is a function of our location in the passband, this also ensures that $\beta=\beta(P_0,\omega_0)+O[(\delta p)^2]$. Mathematically, this is merely an exercise in partial derivatives that yields

$$\omega_P=-\beta_P/\beta_\omega \Rightarrow\beta_\omega\delta\omega=-\beta_P\delta p. \quad (13)$$

Consequently, only $O[(\delta p)^2]$ contributions from Δ^6 remain in (10). Typically, $\omega_P/\omega_0\sim10^{-4}$ mm/mW and has a negligible effect on I'. Thus, assuming $\xi\ll\omega_P/\omega_0$,

$$I'=\lambda^2\tau_0^2\Delta_0^6\left(1+\xi\delta p-\frac{\omega_P}{\omega_0}(1+\xi P_0)\delta p\right)+O[(\delta p)^2] \approx\lambda^2\tau_0^2\Delta_0^6(1+\xi\delta p). \quad (14)$$

Since $I'\propto I/P$, the linear term in (14) represents a quadratic term in $|\kappa|^2$ which in turn is a measure of the quadratic power dependence in m_ρ^2 Thus, an experiment that measures the linear dependence of I' can be used to study the manner in which microwave power affects the dynamic magnetization of forward volume MSWs.

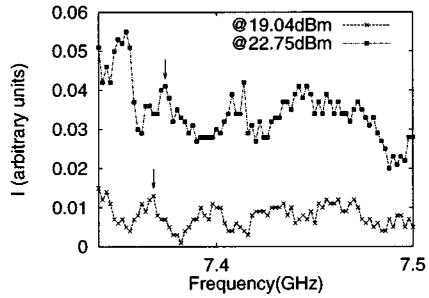

FIG. 2. MSW–optical interaction spectrum for different input microwave power levels. The arrow marks a particular feature in the spectrum that shifts with an increase in power.

III. EXPERIMENTAL RESULTS

Figure 2 shows the interaction spectrum at two different power levels with the arrows marking a particular feature in the spectrum. We monitor the height of the peak marked by the arrow as we increase the input microwave power from 16.6 to 26.7 dB m in steps of 0.1 dB. These power levels are measured as the total power fed into the device. Assuming a perfectly matched and lossless bidirectional transducer 10 mm long, this is 20 times the quantity defined as P in Sec. II B. The normalized intensity I' is shown in Fig. 3 and has been fit to a straight line. A shift in the interaction spectrum of 1.1 MHz mm/mW was determined by studying a density plot of the data over a wide range of frequencies and power levels.[10] The microwave signal was generated using a sweep oscillator that has a plug-in with an accuracy of ±0.5 dB. The finite accuracy will change P_0(mW/mm) by a constant factor. However, we are concerned only with the slope of the line and our analysis is limited by the ±0.01 dB resolution of our input microwave power. Since we had to normalize our measured signal with respect to the input power to obtain I', the resolution of the x axis in Fig. 3 puts a lower bound on any correction terms we may obtain from our analysis of

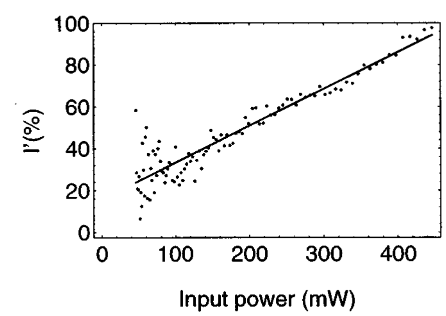

FIG. 3. Experimental variations in the normalized optical intensity (I') as we follow the peak marked in Fig. 2. The data was divided by its maximum value and then fit by the method of least-squares to the straight line $y=15.8(1+0.011x)$ with $\chi^2=0.88$, where x is a measure of the input power fed into the device.

the above data. However, the observed linear dependence in Fig. 3 is too large an effect to be attributed to the finite resolution of our power source.

To facilitate a comparison with the theory in Sec. II B, we need to rescale the x axis by a factor of 20, thereby converting the power levels into units of mW/mm for MSWs on one side of our transducer. With $P_0 = 2.3$ mW/mm (16.6 dB m fed into the transducer), the experimentally obtained linear fit can be rewritten in the form $I' = 23.8(1 + 0.14\delta p)$. Comparing this line with the theoretical expression in (14), we obtain $\xi \sim 0.14$ mm/mW. Since $\tau^2 \xi$ was introduced as the coefficient of P^2 in our expression for m_ρ^2, we find that the MSW–optical interaction can be used to measure the quadratic power dependence in the dynamic magnetization.

IV. THERMAL EFFECTS

The propagation loss for MSWs causes a significant heating of the sample at high microwave power levels. This reduces the saturation demagnetization of the film causing the MSW passband to shift upwards in frequency. The shift depends on the orientation of the sample in the external magnetic field and is ~ 8 MHz/ °C for forward volume MSWs.[11] Since this effect is very similar to the frequency shift observed in the MSW–optical interaction, it is worthwhile for us to estimate the temperature of the film close to the microwave transducer.

The shift in the MSW passband, $\omega_P \delta p$, was measured first as we increased the input microwave power by 20 dB, in steps of 0.1 dB, and then as we decreased it. There was no evidence of any transient thermal behavior when we compared the data recorded in the two experiments. The data shown in Sec. III was obtained with a time constant of 10 s on the lock-in amplifier. The thermal time constant of the sample appeared to be much shorter than the characteristic time constants of our experiment. Therefore, we focus our attention on evaluating the steady state thermal behavior. The substrate has a thickness $d_s = 500$ μm while the film is a mere 6.3 μm. Although most of the heat is generated by the dissipation of MSWs in the film, the steady state thermal behavior is likely to be dominated by the thermal characteristics of the gadolinium gallium garnet (GGG) substrate.

To maximize the MSW–optical interaction, the film is aligned so that the optical beam passes close to the transducer. Any thermal effects observed in the MSW–optical interaction are dominated by the temperature of the film beneath the transducer. A schematic of the assumed temperature profile in the substrate is shown in Fig. 4. It is reasonable to assume that the temperature of the film is a maximum close to the transducer where the power dissipated in the film is a maximum, or equivalently, $(\partial T/\partial y)_{y\to 0} = 0$. We note that there is an air gap between the microstrip circuit and the film and we choose to neglect the heat lost to the surroundings by convection along $+\hat{x}$. Consequently, the heat flow $H = -\nabla T$ at the transducer is directed into the substrate along $-\hat{x}$. With a room temperature T_0 on the other side of the substrate, we now have a simple conduction problem, as shown in Fig. 5, for a segment of the substrate with thickness

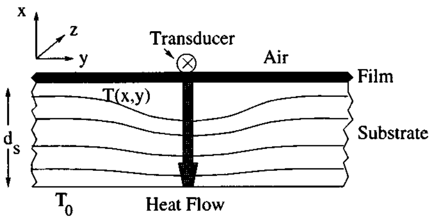

FIG. 4. Schematic showing the assumed temperature profile in the GGG substrate. The heat flow close to the transducer is directed in the $-\hat{x}$ direction.

d_s, width δy, length $2L$ and conductivity[12] $k = 8.5$ W m^{-1}K^{-1}. As a reminder, δP shown in Fig. 5 has units of power per unit length and is consistent with our definition of P in earlier sections.

The power per unit length, δP, is dissipated in a width δy beneath the transducer. The thermal conduction is expressed mathematically in the form

$$\delta P = \frac{k}{d_s}(T - T_0)\,\delta y. \tag{15}$$

The power per unit length associated with MSWs propagating away from a bidirectional transducer is described by $P(y) = P_0 e^{-\alpha|y|}$, where $\alpha = 7.2$ cm^{-1} (31.3 dB/cm) is the decay constant for this film.[4] Since the derivative of P is undefined at $y = 0$, we calculate the change in power beneath the transducer as the sum of the power lost in a width $\delta y/2$ on either side of the transducer. With equal amounts of power lost on both sides, we find

$$\delta P = 2 \cdot \frac{\delta y}{2}\left(\frac{dP}{dy}\right)_{y\to 0^+} = \alpha P_0 \delta y. \tag{16}$$

Combining (15) and (16), we obtain the temperature difference

$$T_{y\to 0} - T_0 = \frac{\alpha P_0 d_s}{k}. \tag{17}$$

We can now estimate the effects of thermal demagnetization in the film as follows:

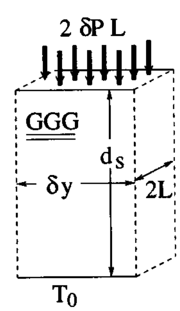

FIG. 5. Characteristic lengths and boundary conditions for thermal conduction beneath the transducer. δP is defined in units of power per unit length.

$$\left(\frac{d\omega}{dP}\right)_{m_\rho}=\left(\frac{d\omega}{dT}\frac{dT}{dP}\right)_{m_\rho}\approx 2\pi(0.17\ \text{MHz-mm/mW}). \tag{18}$$

This shift is comparable to the frequency shift of $2\pi(0.44$ MHz mm/mW) obtained by evaluating (12) at $\omega_0=2\pi(7.3$ GHz).

The model described above is extremely simple and only allows us to estimate the order of magnitude of the thermal demagnetization in our experiment. It does however indicate that the influence of thermal effects in this experimental geometry cannot be entirely ignored. Since ω_P in Sec. III was obtained by following the experimentally observed shift in the interaction spectrum, it undoubtedly measures a frequency shift that results from a combination of increasing dynamic magnetization and thermal demagnetization.

V. CHANGES IN MSW PASSBAND

The addition of a quadratic power term in the dynamic magnetization allows us to calculate the higher order corrections to the MSW dispersion relation. The inclusion of terms of $O(P_0^2)$ in this equation allows us to estimate the dynamic magnetization of circularly polarized MSWs near the bottom edge of the passband.

In an external magnetic field H_{dc}, the edge of the passband is given by $\omega_0=-\gamma\mu_0(H_{dc}-M_s\cos\theta)\equiv\omega_{dc}-\omega_M\cos\theta$, where $\sin\theta=m_\rho/M_s$. With $m_\rho \ll M_s$, the dependence on θ can be expressed as

$$\cos\theta=\sqrt{1-\sin^2\theta}\approx 1-\frac{1}{2}\left(\frac{m_\rho}{M_s}\right)^2+\frac{1}{8}\left(\frac{m_\rho}{M_s}\right)^4. \tag{19}$$

At the edge of the passband, $\beta=0$ and we are primarily interested in the shift in the passband as we increase the power without a change in the wave number. To obtain the $O(P_0^2)$ dependence of ω_0, we once again use a Taylor series expansion, this time expanding $\omega_0(P)$ near P_0. The expansion yields,

$$\omega_0(P)=\omega(P_0)+\omega_0'\delta p+\frac{\omega_0''}{2}(\delta p)^2+O[(\delta p)^3]. \tag{20}$$

Evaluating the derivatives using (6) and retaining only the lowest order terms each time, we find

$$\omega_0'=\left(\frac{\partial\omega_0}{\partial P}\right)_{P_0}=\frac{\omega_M\tau^2}{2M_s^2}+O(\xi P_0), \tag{21}$$

$$\omega_0''=\left(\frac{\partial^2\omega_0}{\partial P^2}\right)_{P_0}=\frac{\omega_M\tau^2}{M_s^2}\left(\xi-\frac{\tau^2}{4M_s^2}\right)+O(\xi P_0). \tag{22}$$

The first derivative ω_0' is merely the linear shift in the passband that was calculated in (11) and its lowest order term remains unchanged. The inclusion of $O(\xi P_0)$ terms in ω_0' gives us a slightly larger linear shift in the passband, but at our operating power levels, it continues to be of the same order of magnitude. In the presence of thermal demagnetization, measuring an increase in ω' to check our estimate for ξ is an experimentally daunting task. However, with values of $\tau^2/M_s^2\sim 10^{-4}$ mm/mW and $\xi\sim 10^{-1}$ mm/mW, the dominant contribution to ω_0'' is due to ξ. Clearly, experiments that directly or indirectly measure ω_0'' will confirm the existence of ξ. An understanding of the nonlinear power dependence in m_ρ will prove crucial as we begin designing high power MSW and MSW–optical devices.

Experimenters working with yttrium–iron garnet films have reported saturation effects in the linear shift of the passband.[3] Our observations on the transverse MSW–optical interaction using a $[BiLu]_3Fe_5O_{12}$ film do not indicate such a saturation. This film has an unusually large ferromagnetic resonance linewidth of ~ 3 Oe. Consequently, the Suhl instability threshold at the main resonance is at a higher power level. Increasing the input power above the threshold can cause the parametric excitation of spin-waves leading to an apparent reduction in the dynamic magnetization at the operating frequency. By staying below the threshold, we effectively rule out such a phenomenon in our experiments.

VI. CONCLUSIONS

We have observed a quadratic power dependence in the transverse MSW–optical interaction using a T-transducer. The solutions to the coupled mode theory for TM→TE conversion were suitably modified to describe the T-transducer geometry. After correcting for the lowest order nonlinear frequency shift in the interaction spectrum, we attribute the residual power dependence of the interaction signal to a quadratic correction in the dynamic magnetization. This is shown mathematically using Taylor series expansions for the MSW wave number and the magneto-optic coupling coefficient.

The quadratic power coefficient is about 0.1 mm/mW times the linear coefficient in our expansion for the dynamic magnetization. The resulting correction to m_ρ will gain importance as we move into a regime where the shift in the MSW passband is no longer linearly dependent on power. More importantly, our results indicate a need to design new experiments that can measure the parameter ω_0'' in the dispersion relation. This would confirm our current estimates for the nonlinear power dependence in the dynamic magnetization. The magnitude of ξ can significantly affect the performance of high power MSW and MSW-optical devices.

We have also estimated the effects of thermal demagnetization in our experiment and show that it is comparable to the effect of increasing the dynamic magnetization at a constant temperature. Further experiments are necessary in order to completely isolate the two phenomena.

ACKNOWLEDGMENTS

We would like to express our gratitude to J. Peruyero for providing us with the BLIG film used in this experiment, to C. E. Patton for drawing our attention to the peculiarities of a T-transducer, to P. Kabos for raising the issue of thermal demagnetization, and to S. Prem Kumar for many discussions on the theoretical and experimental aspects of our device. This research was supported in part by the National Science Foundation under Grant No. ECS-9206817.

APPENDIX

The Cotton–Mouton tensor has been worked out by Prokhorov *et al.*[13] In the case of forward volume MSWs, with the external field along $\hat{x}$, the magnetization can be approximated by

$$\boldsymbol{M}=\hat{x}M_s+\hat{y}m_y(t)+\hat{z}m_z(t), \tag{A1}$$

where m_y and m_z are small signal perturbations of the direction of $\boldsymbol{M}$. We are primarily interested in the tensor element ϵ_{yx} that couples the TM and TE optical modes for the geometry shown in Fig. 1. The effects of the Cotton–Mouton tensor for the collinear MSW–optical interaction up to $O(m_\rho)$ were previously calculated.[9,14] We now extend that calculation to include $O(m_\rho^2)$ terms in the transverse interaction geometry. The relative permittivity tensor element is given by

$$\epsilon_{yx}=-jfm_z+2\left(g_{44}+\frac{\Delta g}{3}\right)M_s m_y+\frac{\Delta g}{3}(m_z^2-m_y^2). \tag{A2}$$

Typical values for the Cotton–Mouton coefficients in SI units are[14–16] $\Delta g M_s^2\sim 0.0002$ and $g_{44}M_s^2\sim -0.0004$. For a BiLuIG film with refractive index $n=2.2$, at $\lambda_0=1.32$ μm, a generous estimate of the Faraday rotation $\Phi_F=fM_s\pi/\lambda_0 n=-2300°/\text{cm}$.[14,17]

The coupling coefficient is expressed as an integral

$$\kappa=-j\frac{\beta_{TM}}{8n^2}\int_{-\infty}^{\infty}dx e_y(x)\epsilon_{yx}h_y(x), \tag{A3}$$

where e_y and h_y are the optical mode fields. The integral is simplified considerably if we assume that the magnetization is approximately constant through the film and is zero elsewhere. Also assuming tightly bound optical modes, the fields for the lowest order modes are

$$e_y(x)=2\sqrt{\frac{\omega_{\text{opt}}\mu_0}{\beta_{TE}d}}\cos\left(\frac{\pi x}{d}\right),$$
$$h_y(x)=2\sqrt{\frac{\omega_{\text{opt}}\epsilon}{\beta_{TM}d}}\cos\left(\frac{\pi x}{d}\right), \tag{A4}$$

and with $\beta_{TE}\approx\beta_{TM}$,

$$\int_{-d/2}^{d/2}dx e_y(x)h_y(x)=2\sqrt{\epsilon_r}=2n. \tag{A5}$$

For forward volume MSWs associated with a frequency ω and propagating in the $+\hat{y}$ direction, the ratio of the components of the dynamic magnetization is given by[8]

$$\frac{m_y}{m_z}=-j\frac{\omega_0}{\omega}, \tag{A6}$$

where ω_0 is the frequency associated with the bottom edge of the passband. Combining (A2), (A3) and (A6), we obtain

$$|\kappa|^2=\left(\frac{\Phi_F-\Phi_{CM}^{(1)}}{2}\right)^2\left(\frac{m_z}{M_s}\right)^2+\left(\frac{\Phi_{CM}^{(2)}}{4}\right)^2\left[1-\left(\frac{\omega_0}{\omega}\right)^2\right]^2\left(\frac{m_z}{M_s}\right)^4, \tag{A7}$$

where $\Phi_{CM}^{(1)}=[g_{44}+(\Delta g/3)]2M_s^2\pi/\lambda_0 n$ and $\Phi_{CM}^{(2)}=\sqrt{2}\Delta g\times M_s^2\pi/3\lambda_0 n$. By staying close to the edge of the passband, the $O(m_z^4)$ term vanishes. In our experiment, $\omega=2\pi$ (7.37 GHz) and $\omega_0=2\pi$ (7.30 GHz) and the second term is six orders of magnitude smaller than the first term at our maximum input microwave power of 440 mW. Hence, we can neglect the $O(m_z^4)$ term in (A7).

1. A. D. Fisher, E. S. Gaynor, and J. Lee, IEEE Ultrason. Symp. **1**, 226 (1983).
2. C. S. Tsai, D. Young, W. Chen, L. Adkins, C. C. Lee, and H. Glass, Appl. Phys. Lett. **47**, 651 (1985).
3. M. A. Tsankov, M. Chen, and C. E. Patton, J. Appl. Phys. **79**, 1595 (1996).
4. A. Cash and D. D. Stancil, IEEE Trans. Magn. **32**, 5188 (1996).
5. L. Li, K. Yashiro, and S. Ohkawa, IEEE Trans. Magn. **32**, 4168 (1996).
6. A. A. Stashkevich, M. G. Cottam, and A. N. Slavin, J. Appl. Phys. **79**, 5371 (1996).
7. A. Yariv, IEEE J. Quantum Electron. **QE-9**, 919 (1973).
8. D. D. Stancil, *Theory of Magnetostatic Waves* (Springer, New York, 1993), Ch. 7.
9. D. D. Stancil and N. Bilanuik, in *High Frequency Processes in Magnetic Materials,* edited by G. Srinivasan and A. Slavin (World Scientific, Singapore, 1995).
10. A. Prabhakar and D. D. Stancil, IEEE Trans. Magn. **32**, 4174 (1996).
11. W. S. Ishak, Proc. IEEE **76**, 171 (1988).
12. P. A. Popov, A. V. Antonov, I. A. Ivanov, and A. A. Sidorov, Sov. Phys. Solid State **31**, 1820 (1989).
13. A. M. Prokhorov, G. A. Smolenskii, and A. N. Ageev, Sov. Phys. Usp. **27**, 339 (1984).
14. D. D. Stancil, IEEE J. Quantum Electron. **27**, 61 (1991).
15. R. V. Pisarev, I. G. Sinii, N. N. Kolpakova, and Y. M. Yakovlev, Sov. Phys. JETP **33**, 1175 (1971).
16. K. Ando, N. Koshizuka, T. Okuda, and Y. Yokoyama, Jpn. J. Appl. Phys. **22**, L618 (1983).
17. H. Tamada, M. Kaneko, and T. Okamoto, J. Appl. Phys. **64**, 554 (1988).